In Figure 3(a), the total field observed just in front of the scattering strip is plotted versus frequency, normalised to the maximum frequency in the simulation ($0.5/\Delta_t$, with $\Delta_t$ the simulation time step). The strip-TLM results are compared to both the analytic results as well as those from a wire-TLM simulation, where a round wire of diameter equal to the width of the metal strip has been used instead [5]. It is clear that the accuracy obtained with the strip-TLM model is excellent over a wide range of frequencies. Furthermore, it is noted that the large-scale consequences of the different nature of the fields close to the wire and strip are clearly apparent, even at moderate frequencies. Attention is particularly drawn to the fact that at higher frequencies the small difference in the phase of the reflected field (due to the fact that the front of the wire is slightly closer to the observation point) is detected, even though this distance is smaller than the node size. In Figure 3(b), the field that penetrates through a narrow slot is plotted versus normalised frequency, expressed in the form of the shielding effectiveness ($-20 \log |E|$, where $E$ is the observed field for unit amplitude excitation). To demonstrate how accurate the approach is, results are also shown for the case where the slot is modelled without the special slot node, but by just using one full-width conventional TLM node to model the slot. It is seen that even for the 4-cm-wide slot (80% of the node width), the special node model clearly provides more accurate results than when the slot is quantised to a full node width. This effect is far more dramatic for the case of a 1-cm-wide slot (20% of the node width); the special node model still demonstrates extremely good agreement with the analytical results and now the full node-width approximation is 8-dB in error.

Finally, although the results presented in this paper are for the TM polarised case, it is pointed out that it is straightforward to develop the TE case in the same manner.

### 3. CONCLUSION

A highly accurate method for embedding thin conducting flat strips and narrow slots in conducting planes for transmission-line model (TLM) simulations has been demonstrated. Verification of the model with the analytic results has proved the approach to be extremely accurate. The significance of this model is that it allows substantial savings in both run time and memory to be achieved as compared to simulations that directly resolve these features by fine meshing, which will be of particular importance in the realm of EMC where a wide range of physical scales is a common occurrence.

### REFERENCES


1. C. Christopoulos, The transmission-line modelling method: TLM, IEEE Press, Piscataway, NJ, 1995.
2. C. Christopoulos, Multiscale modeling in time-domain electromagnetics, Int J Electron Commun 57 (2003), 100–110.
3. P. Sewell, J.G. Wykes, T.M. Benson, C. Christopoulos, D.W.P. Thomas, and A. Vukovic, Transmission-line modelling using unstructured triangular meshes, IEEE Trans Microwave Theory Tech 52 (2004), 1490–1497.
4. Y.K. Choong, P. Sewell, and C. Christopoulos, Accurate wire representation in numerical models for high-frequency simulation, Electron Lett 37 (2001), 280–282.
5. P. Sewell, Y.K. Choong, and C. Christopoulos, An accurate thin-wire model for 3D TLM simulations, IEEE Trans Electromag Compat 45 (2003), 207–217.
6. Y. Liu, P. Sewell, K. Biwojno, and C. Christopoulos, A generalized node for embedding sub-wavelength objects into 3D transmission-line models, IEEE Trans Electromag Compat (to appear).
7. Y. Liu, K. Biwojno, P. Sewell, and C. Christopoulos, A general approach for embedding local-field solutions into TLM simulations, XXVIII Gen Assem Union of Radio Sci (URSI), Delhi, 2005, (to appear).
8. P. Morse and H. Feshbach, Methods of theoretical physics, McGraw Hill, New York, 1953.




---

# MICROWAVE STUDIES OF A POLY VINYL ACETATE (PVA)-BASED PHANTOM FOR APPLICATIONS IN MEDICAL IMAGING

**G. Bindu, Vinu Thomas, Anil Lonappan, C. K. Aanandan, and K. T. Mathew**
Department of Electronics
Microwave Tomography and Materials Research Laboratory
Cochin University of Science and Technology
Kochi–682 022, India

*Received 18 July 2005*

**ABSTRACT:** *A phantom that exhibits complex dielectric properties similar to low-water-content biological tissues over the electromagnetic spectrum of 2000–3000 MHz has been synthesized from carbon black, graphite powder, and poly vinyl acetate (PVA)-based adhesive. The material overcomes various problems that are inherent in conventional phantoms such as decomposition and deterioration due to the invasion of bacteria or mold. The absorption coefficients of the material for various concentrations of carbon and graphite are studied. A combination of 50% poly-vinyl-acetate-based adhesive, 20% carbon, and 30% graphite exhibits a high absorption coefficient, which suggests another application of the material as a good microwave absorber for the interior lining of tomographic chamber in microwave imaging. The cavity-perturbation technique is adopted to study the dielectric properties of the material.* © 2005 Wiley Periodicals, Inc. Microwave Opt Technol Lett 48: 180–183, 2006; Published online in Wiley InterScience (www.interscience.wiley.com). DOI 10.1002/mop.21300

**Key words:** *dielectric constant; microwave imaging; cavity-perturbation technique; absorbing material*

### INTRODUCTION

Microwave tomography is one of the most challenging and advanced technologies, with enormous potential applications in the field of medical imaging. Microwave images are maps of the electrical-property distributions in the body. At microwave frequencies, biological-tissue interactions with the fields are defined by their complex relative permittivity. The bound water content of the tissues is a major factor in determining the permittivity [1].

Many prototypes of active microwave imaging setups have been presented [2, 3]. Evaluation of the performance of these prototypes requires imaging and interpretation of test objects or phantoms [4]. These could be simple uniform blocks or steps, or more complex designs containing embedded objects, in order to provide tests of resolution or shape detection. It is desirable that the material should respond to microwaves in a similar fashion to the anatomical areas they represent, particularly in tests which measure or calibrate microwave exposures, or when used for optimization of system parameters over the required frequency range. The dielectric properties of the tissue-equivalent materials should yield a close match to the actual tissue conditions. Also, the material should be well adapted when intermediate compositions are desired.

Various types of phantoms are already in use as tissue substitutes for microwave medical imaging [5, 6]. These compounds are constructed in one of two ways: the first consists of a jelly agent, polyethylene powder, sodium chloride, and water, and the second consists of agar, sodium chloride, and water. The disadvantage of constructing a phantom model using these materials is that the models cannot be used repeatedly, as they dry out and decompose over time. To avoid this, nonhydrated phantom models are made of ceramic [7] to simulate muscle tissue. However, these models require a specific adhesive made of ceramic powder, whose function is to remove any air gaps between adjacent pieces of ceramic. Unfortunately, the adhesive is difficult to use and the hard ceramic material cannot be cut or reshaped easily.

This paper presents a nonhydrated phantom model that overcomes the shortcomings of conventional phantoms. The material is composed of a polyvinyl acetate (PVA)-based adhesive, carbon, and graphite powder. The complex relative permittivity of the phantom model can be controlled by adjusting the composition ratio in order to simulate various biological tissues. The absorption coefficient of the material is studied for its feasibility of using as microwave absorbing material for coating the interior of microwave tomographic chamber. A frequency of 2000–3000 MHz is selected for the study to conveniently include the industrial, scientific, and medical (ISM) applications band of 2450 MHz.

## EXPERIMENTAL SETUP AND PROCEDURE

The samples are prepared by mixing PVA-based adhesive carbon and graphite in different known proportions. PVA is cheap and commercially available under the brand name Fevicol. Pellets of the samples are made for various carbon to graphite ratios of 50:0, 40:10, 30:20, 20:30, 10:40, and 0:50, with the PVA content in all the samples fixed as 50%. It is found that if the PVA content is more than 50%, there is difficulty in setting the compound. Microwave studies of the samples have been done using cavity-perturbation technique [8].

The experimental setup consists of a transmission-type S-band rectangular cavity resonator, an HP 8714 ET network analyzer, and an interfacing computer, as shown in Figure 1(a). The cavity is made from S-band wave guide with both ends closed. Figure 1(b) shows the schematic diagram of the cavity resonator. The length of the resonator determines the number of resonant frequencies. The transmission-type resonator used in this experiment is excited in the $TE_{10p}$ mode. The resonant frequency $f_o$ and the corresponding quality factor $Q_o$ of each resonant peak of the empty cavity resonator at the maximum of electric field are noted. The pellets are introduced into the cavity resonator through the nonradiating slot. The resonant frequencies of the sample-loaded cavity are selected and the position of the sample is adjusted for maximum perturbation (that is, maximum shift of resonant frequency with minimum amplitude for the peak). The new resonant frequency $f_s$ and the quality factor $Q_s$ are determined. The procedure is repeated for the other resonant frequencies.

## THEORY OF CAVITY PERTURBATION

When a material is introduced into a resonant cavity, the cavity-field distribution and resonant frequency are changed, depending on the geometry, electromagnetic properties, and position of the sample in the fields of the cavity. Dielectric material interacts only with electric field in the cavity.

According to the theory of cavity perturbation, the real and imaginary parts of the complex relative permittivity [8] can be expressed as

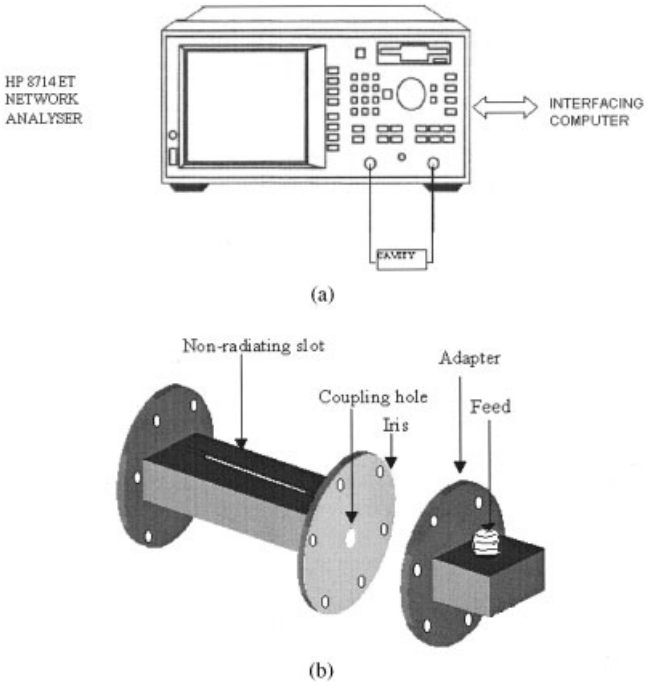


**Figure 1** (a) Experimental setup; (b) schematic diagram of the cavity resonator

$$\varepsilon_r' - 1 = \frac{f_o - f_s}{2f_o}\left[\frac{V_c}{V_s}\right], \tag{1}$$

$$\varepsilon_r'' = \frac{V_c}{4V_s}\left(\frac{Q_o - Q_s}{Q_o Q_s}\right), \tag{2}$$

where $\varepsilon_r'$ is the real part of the complex relative permittivity (known as the dielectric constant), $\varepsilon_r''$ is the imaginary part of the complex relative permittivity associated with the dielectric loss of the material, and $V_s$ and $V_c$ are the volumes of the sample and the cavity resonator, respectively. The conductivity can be related to the imaginary part of the complex relative permittivity as follows:

$$\sigma_e = \omega\varepsilon'' = 2\pi f_s \varepsilon_0 \varepsilon_r''. \tag{3}$$

The absorption coefficient $\alpha$ of the material is given by

$$\alpha = \frac{\pi\varepsilon_r'' f_s}{c\sqrt{(\varepsilon_r'^2 + \varepsilon_r''^2)}}, \tag{4}$$

where $n$ is the real part of the complex refractive index given by $n = \sqrt{\varepsilon_r'}$ and $c$ is the velocity of light in free space.

## RESULTS AND DISCUSSION

In the frequency range of 2000–3000 MHz, carbon, graphite, and PVA exhibited dielectric constant variations from 3.8 to 2.67, 4.8 to 3.87, and 5.74 to 4.02, respectively. For the same frequency range, the conductivity variations are from 0.024 to 0.067, 0.003 to 0.005, and 0.003 to 0.015, respectively. When these materials are mixed in definite proportions, the dielectric constant and conductivity increases from their respective elemental values and behaves as an ideal simulant of low-water-content biological tissues.

The variations of dielectric constant and conductivity with frequency for various combinations of carbon, graphite, and PVA are shown in Figures 2 and 3. It is observed that for all the phantom

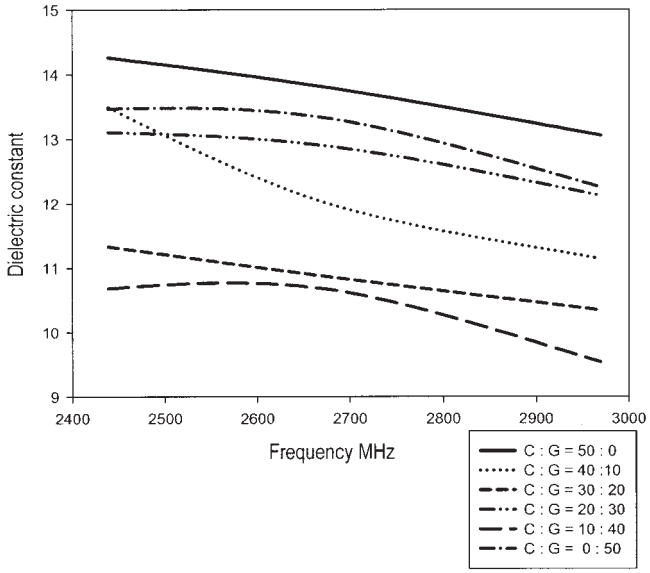


**Figure 2** Variation of dielectric constant with frequency for the phantom (C: carbon, G: graphite powder)

samples, the dielectric constant decreases and conductivity increases, with an increase in frequency. This result coincides with the studies on dielectric properties of biological tissues [9].

The observed decrease of dielectric constant with an increase in frequency that may be due to the orientation of the polarization in the microwave field. The higher the polarizability of the material, the greater the dielectric constant. In the case of orientation polarization, the applied field causes a net orientation of the dipoles parallel to the field. At sufficiently low frequencies, all three types (electronic, atomic, and orientation) of polarization take place. As the frequency of the applied field is increased, the net polarization is reduced due to orientation polarization and total polarizability falls to $\alpha_T - \alpha_O$, where $\alpha_T$ is the total polarizability and $\alpha_O$ is the polarizability of orientation polarization [10]. This fall in polarizability leads to dielectric relaxation which, in turn, leads to a

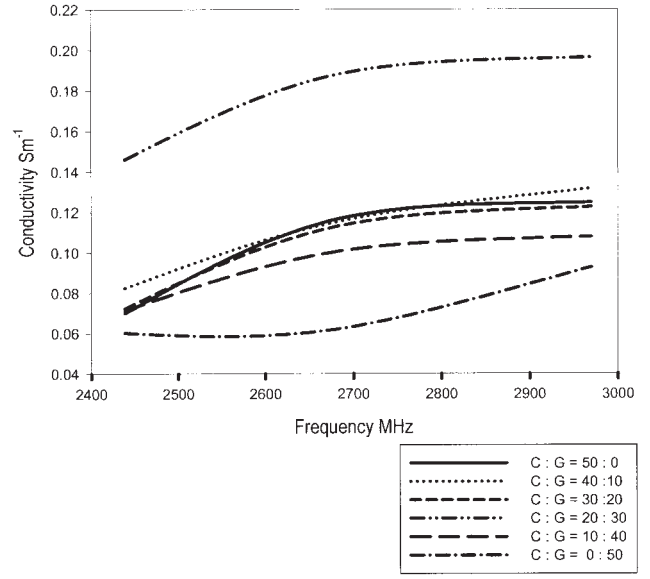


**Figure 3** Variation of conductivity with frequency for phantom (C: carbon, G: graphite)

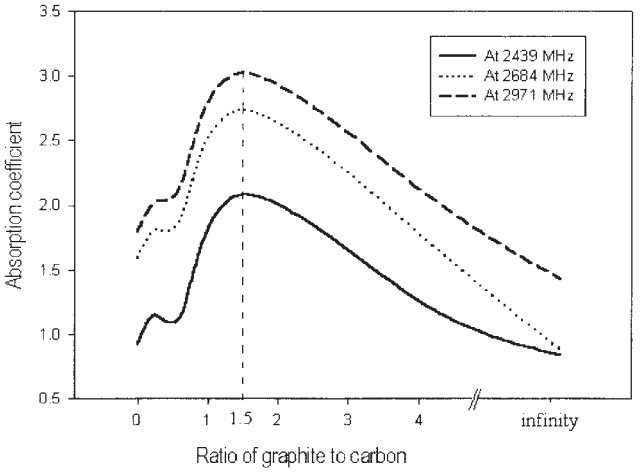


**Figure 4** Variation of absorption coefficient for different compositions of carbon and graphite (in all the samples PVA constitutes 50% of the composition)

decrease in dielectric constant. In other words, at higher frequencies, due to the rotational displacement of polar groups under the influence of the electric field, frictional loss increases and reduces the dielectric constant.

The conductivity of dielectric materials in a microwave field depends upon the dielectric loss factor $\varepsilon''_r$. As frequency increases, the dielectric loss factor increases. The dielectric loss is a direct function of the relaxation process, which is due to the local motion of the polar groups. At high frequencies, the friction between the molecular chains increases, which leads to a higher dielectric loss. This dielectric-loss factor leads to the so-called "conductivity relaxation." At the relaxation region, the polarization acquires a component out-of-phase with the field and a displacement current in-phase with the field, resulting in thermal dissipation of energy. This generates dielectric loss which in turn generates conductivity.

When carbon, graphite, and PVA are mixed in definite proportions, the conductivity and dielectric constant increases, compared to their corresponding elemental values, due to interfacial polarization. In heterogeneous dielectrics where a dielectric material is composed of two or more phases, space-charge build up occurs at the macroscopic interface as a result of the differences in the conductivities and dielectric constants of the materials at the interface. This accumulation of space charge leads to field distortions and dielectric loss; this interfacial loss depends on the quantity of filler present, as well as on the geometrical shape of its dispersion. The magnitude of the interfacial loss is particularly susceptible to the length of the dispersed phase geometry in the direction of the field. Due to this interfacial loss, the conductivity increases [10]. Also, in the presence of a microwave field, the dielectric constant depends on the dipolar polarization as well. The accumulation of polar charges at the interface leads to dipolar polarization, which in turn increases the dielectric constant.

The absorption coefficient of the material depends on dielectric constant, conductivity, and resonant frequency $f_s$, as given in Eq. (4). The absorption coefficients of the samples are plotted versus the composition ratios of graphite to carbon shown in Figure 4. It is observed that a combination of 50% PVA, 20% carbon, and 30% graphite exhibits good absorption rate and is ideal for use as microwave-absorbing material in microwave tomographic imaging.

The equivalent phantoms for various low-water-content biological samples [11] in the frequency range of 2000–3000 MHz is

**TABLE 1 Equivalent Phantoms of Various Biological Tissues in the Frequency Range of 2000–3000 MHz**

| Biological Sample | Range of Dielectric Constant | Range of Conductivity [$Sm^{-1}$] | Equivalent Phantom Ratio of Carbon to Graphite with 50% PVA |
|---|---|---|---|
| Bladder, human | 13.5–13.1 | 0.21–0.215 | C:G = 40:10,C:G = 0:50 |
| Breast fat, human | 10.2–9.8 | 0.052–0.062 | C:G = 10:40 |
| Bone (cancellous), human | 12.6–12.14 | 0.15–0.17 | C:G = 20:30 |
| Bone (cortical), ovine | 11.78–11.299 | 0.17–0.23 | C:G = 30:20 |
| Bone (cortical), human | 12.44–10.96 | 0.068–0.71 | C:G = 20:30 |
| Bone marrow (infiltrated), ovine | 14.76–13.31 | 0.175–0.182 | C:G = 50:0 |

given in Table 1. It is observed that phantoms of any of these biological tissues can be simulated by mixing carbon and graphite powder in definite proportions with PVA.

## CONCLUSION

A PVA-based composite of carbon and graphite has been identified as a suitable phantom material for microwave medical imaging. The dielectric constant and conductivity of this material exhibit good matching with the available literature data on biological tissues. The high value of the absorption coefficient of the material underlies its application as microwave-absorbing material in medical imaging.


## ACKNOWLEDGMENT

Authors G. Bindu and A. Lonappan thankfully acknowledge CSIR, Govt. of India, for providing Senior Research Fellowships.


## REFERENCES


1. S.Y. Semenov, R.H. Svenson, A.E. Boulyshev, A.E. Souvorov, V.Y. Borisov, Y. Sizov, A.N. Staostin, K.R. Dezern, G.P. Tatsis, and V.Y. Baranov, Microwave tomography: Two-dimensional system for biological imaging, IEEE Trans Biomed Engg 43 (1996), 869–877.
2. P.M. Meaney, K.D. Paulsen, A. Hartov, and R.K. Crane, An active microwave imaging system for reconstruction of 2D electrical property distributions, IEEE Trans Biomed Engg 42 (1995), 1017–1026.
3. P.M. Meaney, M.W. Fanning, D. Li, S.P. Poplack, and K.D. Paulsen, A clinical prototype for active microwave imaging of the breast, IEEE Trans Microwave Theory Tech 48 (2000), 1841–1853.
4. J.T. Chang, M.W. Fanning, P.M. Meaney, and K.D. Paulsen, A conductive plastic for simulating biological tissue at microwave frequencies, IEEE Trans Electromagn Compat 42 (2000), 76–81.
5. A.W. Guy, Analyzes of electromagnetic fields induced in biological tissues by thermographic studies on equivalent phantom models, IEEE Trans Microwave Theory Tech MTT-19 (1971), 205–214.
6. T. Matsuda, T. Yoshida, T. Arioka, S. Takatsuka, Y. Nikawa, and M. Kikuchi, Development of 430-MHz microwave heating system by using lens applicator (III): Characteristics of heating, Jpn J Hyperthermic Oncology 12 (1988), 317–329.
7. H. Tamura, Y. Ishikawa, T. Kobayashi, and T. Nojima, Dry phantom material composed of ceramic and graphite powder, IEEE Trans Electromagn Compat 39 (1997), 132–137.
8. K.T. Mathew and U. Raveendranath, Sensors update, Wiley–VCH, Germany, 1999, pp 185–210.
9. S. Gabriel, R.W. Lau, and C. Gabriel, Dielectric properties of biological tissues II: Measurements in the frequency range 10 Hz to 20 GHz, Phys Med Bio 41 (1996), 2251–2269.
10. T.A. Ezquerra, F. Kremmer, and G. Wegner, Progress in electromagnetic research, vol. 6, Elsevier, New York, 1992.
11. S. Gabriel, R.W. Lau, and C. Gabriel, Dielectric properties of biological tissues III: Parametric models for the dielectric spectrum of tissues, Phys Med Bio 41 (1996), 2271–2293.




# CURRENT MODELING OF MICROSTRIP FILTERS


**Odilon M. C. Pereira Filho,[1] Luiz C. da Silva,[2] and Cassio G. do Rego[1]**

[1] Department of Electronics Engineering
Federal University of Minas Gerais
Belo Horizonte, MG 31270-901, Brazil
[2] Center for Telecommunications Studies
Catholic University of Rio de Janeiro
Rio de Janeiro, RJ 22453-900, Brazil


*Received 14 July 2005*


**ABSTRACT:** *This paper presents the current modeling of microwave filters using only entire-domain basis functions. Two sets of entire-domain basis functions are introduced, and their results are compared with the measurements and with those obtained using subdomain basis functions. It also discusses the evaluation of the matrices using the method of moments (MoM).* © 2005 Wiley Periodicals, Inc. Microwave Opt Technol Lett 48: 183–187, 2006; Published online in Wiley InterScience (www.interscience.wiley.com). DOI 10.1002/mop.21301


**Key words:** *microstrip filter; basis functions; method of moments*

## 1. INTRODUCTION

The method of moments (MoM) [1] has been widely used for analyzing microstrip circuits. A key step of the procedure is the choice of the basis functions, which affects the accuracy of the results and the computational efficiency. Subdomain basis functions (rooftops or piecewise sinusoidal) are the most popular choice for modeling the currents on arbitrary microstrip circuits, combined with the delta-gap generator. Although very flexible, they often result in a large number of basis functions and computational effort. Alternatively, the currents may be expanded in a combination of traveling waves at portions of the input and output transmission lines away from discontinuities, and subdomain basis functions in the remainder of the circuit. The traveling-wave portion may be truncated after several cycles [2–6], where the continuity of the current is accomplished by truncating the real part (cosine) a quarter-wavelength from a zero of the imaginary part (sine) [2–4], or by using compensation functions [6]. In [7, 8], semi-infinite traveling waves and subdomain basis functions were used, with the resulting singularities evaluated analytically. The currents may also be expanded exclusively in entire-domain basis functions, in each portion of the circuit, as given in [9] for boxed microwave circuits.

This work explores the physical properties of side-coupled microstrip filters (Fig. 1) in order to propose two sets of entire-domain basis functions, in each portion of the filter, that efficiently model the currents on its surface. The currents on the input and

This work was partially supported by CNPq and FAPEMIG under project TEC-398/04.